Quaternary slip rate and geomorphology of the Alpine fault: Implications for kinematics and seismic hazard in southwest New Zealand

Rupert Sutherland[†]
Kelvin Berryman[‡]
Institute of Geological and Nuclear Sciences, P.O. Box 30-368, Lower Hutt, New Zealand

Richard Norris[§]
University of Otago, P.O. Box 56, Dunedin, New Zealand

ABSTRACT

Glacial landforms at 12 localities in 9 river valleys are offset by the southern end of the onshore Alpine fault. Offsets cluster at ~435, 1240, and 1850 m, consistent with evidence for glacial retreat at 18, 58, and 79 calendar ka. The peak of an offset fluvial aggradation surface is correlated with the Last Glacial Maximum at 22 ka. Displacement rates derived from features aged 18, 22, 58, and 79 cal. ka are 24.2 ± 2.2, 23.2 ± 4.9, 21.4 ± 2.6, and 23.5 ± 2.7 mm/yr, respectively, with uncertainties at the 95% confidence level. The joint probability, weighted mean, and arithmetic mean of all observations pooled by rank are 23.1 ± 1.5, 23.2 ± 1.4, and 23.1 ± 1.7 mm/yr, respectively. We conclude that the mean surface displacement rate for this section of the Alpine fault is 23.1 mm/yr, with standard error in the range of 0.7–0.9 mm/yr. The reduction in estimated long-term slip rate from 26 ± 6 mm/yr to 23 ± 2 mm/yr results in an increase in estimated hazard associated with faulting distributed across the rest of the plate boundary. Model-dependent probabilities of Alpine fault rupture within the next 50 yr are in the range 14%–29%. The 36 ± 3 mm/yr of total plate motion (NUVEL-1A) is partitioned into 23 ± 2 mm/yr of Alpine fault dextral strike slip, 12 ± 4 mm/yr of horizontal motion by clockwise block rotations and oblique dextral-reverse faulting up to 80 km southeast of the Alpine fault, and 5 ± 3 mm/yr of heave on reverse faults at the peripheries of the plate boundary.

Keywords: Alpine fault, tectonics, earthquakes, glacial deposits, plate collision, strike-slip faults.

INTRODUCTION

The Alpine fault is the most obvious geological structure associated with the active Australia-Pacific plate boundary in South Island, New Zealand (Berryman et al., 1992; Norris and Cooper, 2001; Norris et al., 1990). It is a mature dextral strike-slip fault that can be traced for a distance of 900 km (Fig. 1) without any separations of the active fault trace >10 km (Barnes et al., 2001; Berryman et al., 1992; Delteil et al., 1996). The NUVEL-1A plate boundary displacement rate near the Alpine fault varies from 35 mm/yr to 38 mm/yr, depending on position (Fig. 1), and has a 95% confidence interval half-width of 3 mm/yr for rate and 2° for azimuth (DeMets et al., 1994). Geodetic measurements from the central South Island show that motion during the last decade falls within this range (Beavan and Haines, 2001).

Offset late Quaternary deposits show that the Alpine fault accommodates 60%–80% of plate motion in central South Island (Berryman et al., 1992; Norris and Cooper, 2001; Sutherland and Norris, 1995), which is consistent with dislocation models of geodetic strain (Beavan et al., 1999) and estimates based on offset Pliocene sediments (Sutherland, 1994). The Alpine fault displacement rate has significance for any discussion of South Island kinematics or seismic hazard, but the Quaternary rate is constrained by few published data (Norris and Cooper, 2001).

The goals of this paper are to better estimate Alpine fault surface displacement rate, to make a formal attempt at quantifying the uncertainty in rate, and to better constrain the patterns and rates of fault-slip partitioning across the plate boundary. We present an analysis of offset features along an 80 km length of fault trace at the southern end of the onshore Alpine fault (Figs. 1 and 2). We are able to determine the surface displacement rate much more precisely than previous attempts because we take a mean value of 13 individual displacement rate estimates, rather than analyzing each locality in isolation.

The study region is mountainous, with many peak heights in the range of 1000–2000 m, and the Alpine fault is a conspicuous physiographic feature because it offsets topography (Fig. 2). There is no sudden change in mean altitude across the Alpine fault, which is consistent with observations of horizontal or shallowly plunging slickensides on exposed fault surfaces (Berryman et al., 1992; Sutherland and Norris, 1995). In contrast, in the region farther north near Mount Cook (Fig. 1), the Alpine fault dips southeast, has moderately plunging slickensides, and is upthrown to the southeast (Norris and Cooper, 2001; Norris et al., 1990). The relative simplicity of the fault trace in the southern region (Fig. 2) is associated with lower exhumation rates, which have led to superior preservation of offset features on both sides of the Alpine fault.

Valleys with a wide range of geometries cross the Alpine fault in the region studied (Fig. 2; GSA Data Repository material[1]), and offset topography is common. All major valleys draining across the Alpine fault in the southern region have been glaciated since 100 calendar ka, but glaciers are now restricted to small areas around the highest peaks. Valley morphology is largely a result of glacial processes, with later modification by fluvial and landslide processes.

Offset hillslopes, moraines, and a fan were identified using stereo aerial photographs and

[†]E-mail: r.sutherland@gns.cri.nz.
[‡]E-mail: k.berryman@gns.cri.nz.
[§]E-mail: richard.norris@stonebow.otago.ac.nz.

[1]GSA Data Repository item 2006048, details of catchments studied, is available on the Web at http://www.geosociety.org/pubs/ft2006.htm. Requests may also be sent to editing@geosociety.org.

GSA Bulletin; March/April 2006; v. 118; no. 3/4; p. 464–474; doi: 10.1130/B25627.1; 7 figures; 2 tables; Data Repository item 2006048.

field investigations, and then displacements were quantified using 1:50,000 maps (NZMS 260 series). Ages associated with offsets were assigned by correlation with dated deposits in New Zealand and global or South Pacific records. Displacement rates were computed using a Monte-Carlo method that takes into account uncertainties associated with each measurement and any assumed correlations. A GSA Data Repository item (see footnote 1) contains additional supporting data, tables, figures, photographs, and descriptions of methods.

OFFSET MEASUREMENT AND LOCAL CONFIDENCE INTERVAL

Offset glacial landforms are most easily identified from stereo aerial photos that were taken at low altitude. Moraine and till-covered surfaces can be identified by hummocky or linear morphology, and the characteristic poorly drained soils may lead to conspicuous vegetation differences. Newly produced 1:50,000 maps (NZMS 260) are available in digital form, and these digital data were used to measure offsets of landforms.

At least three markers were used to determine Alpine fault offset at each locality. Each marker had components of measurement uncertainty associated with the definition of the marker and extrapolation of the marker to the fault trace. Where offset hillslopes were used, the steepest and least-modified slopes were chosen, and contours were fit with a smooth line through regions that have escaped later fluvial or landslide modification. Extrapolation was based upon geomorphic interpretation, and correlative markers were assumed to have the same trend at their Alpine fault intersection. In some cases, linear markers were identified (e.g., moraine crests at Hokuri Creek), but in most cases, offset hillslopes (surfaces) were used. Glacially formed hillslopes are generally smooth, and hence representative contours were chosen as markers in place of linear features.

At any particular locality, offset between specified minimum and maximum values was considered equally likely (i.e., a rectangular probability density function). The bounding values were determined among all possible values of offset for the three markers (Table 1). Results are reported as a mean offset and inferred 100% confidence interval half-width, C_x (Table 1).

The use of extrapolated markers means that all surface displacement within the principal displacement zone is sampled, even though it may actually be distributed over a width of 10–100 m. The locations of rivers and landslides, and any vertical component of slip across the fault, may affect all offset determinations in a similar fashion, and hence the C_x confidence intervals may not fully account for these correlated uncertainties. Components of vertical slip on the fault are small where they can be measured (fault-plane striations, offset linear markers, or offset subhorizontal surfaces). Where possible, we employed slopes of different aspect on opposing valley sides so that the effects of vertical slip or erosion-deposition along strike of the fault tend to cancel when data are combined into a mean value.

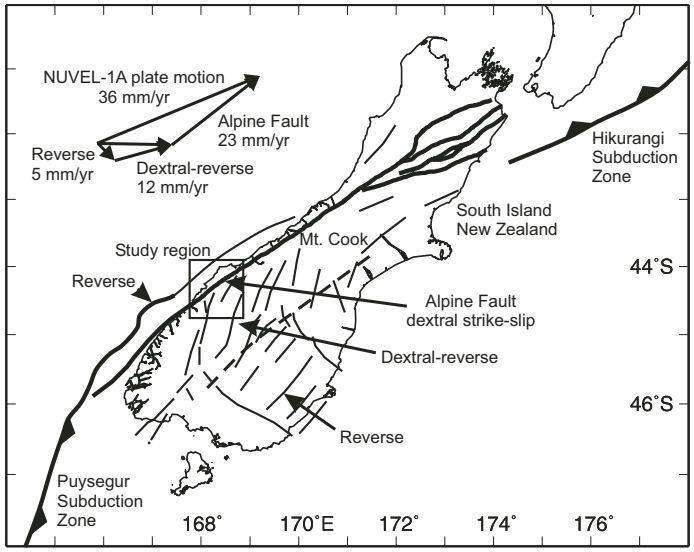

Figure 1. Location of the study area and Alpine fault in South Island, New Zealand. NUVEL-1A plate motion (DeMets et al., 1994) is partitioned into Alpine fault strike-slip and dextral reverse faulting in the zone within 80 km southeast of the Alpine fault, and reverse faulting at the plate boundary peripheries.

STUDY AREA MORPHOLOGY

Martyr Valley and Cascade Moraines

The prominent right step in the Martyr River channel and apparent offset of the valley by the Alpine fault was one of the first features used to infer a Quaternary slip rate of ~25 mm/yr (Clark and Wellman, 1959; Wellman, 1953). Exposure in the northeast bank of Martyr River reveals a steeply southeast-dipping (60°–90°) fault that cuts mylonite, cataclasite, gravel, and silt containing glacial dropstones. Slickenside lineations in parts of the exposure within 10 m of the fault plane plunge shallowly northeast or southwest.

Air photo interpretations and topographic maps show that both sides of the Martyr Valley are offset by a comparable amount to the spur southwest of Martyr River (Fig. 3A). A lateral moraine of the paleo-Cascade glacier aligns to the hillslope upstream, when restored by the same offset (Fig. 3A). The moraine geometry indicates that valley sides at this locality were last scoured by ice when ice levels in the Cascade Valley retreated from an altitude of ~400 m. Mapping of the youngest Cascade Plateau lateral moraines (Fig. 2) demonstrates that an ice thickness of 500–600 m existed here at 19 cal. ka and must predate spur morphology.

Jerry River Valley

The upper part of the Jerry River valley has a smooth cross-valley profile with minimal incision by tributaries, and a lateral moraine that is visible on air photos and in the field provides further evidence for recent glaciation of the catchment. Glacial deposits are also found in the lower reaches of Jerry River, and valley morphology indicates late Quaternary glaciers have extended to near the present coastline. Offset of the valley by the Alpine fault is conspicuous, because the valley is only 1000 m across (Fig. 3B), but it is offset 461 ± 111 m. The relatively large uncertainty in offset arises because no linear feature can be identified, and glaciated surfaces have been modified by fluvial and landslide erosion and deposition. Despite substantial erosion and deposition upstream from the Alpine fault, the offset valley profile was of similar shape prior to fluvial and landslide modification (Fig. 4).

Big Bay and Pyke River Hillslopes

Offset glaciated hillslopes at the northern margin of the Skippers Range were created when ice flowed out to Big Bay (Fig. 3C); lateral moraines on the north side of Big Bay rise

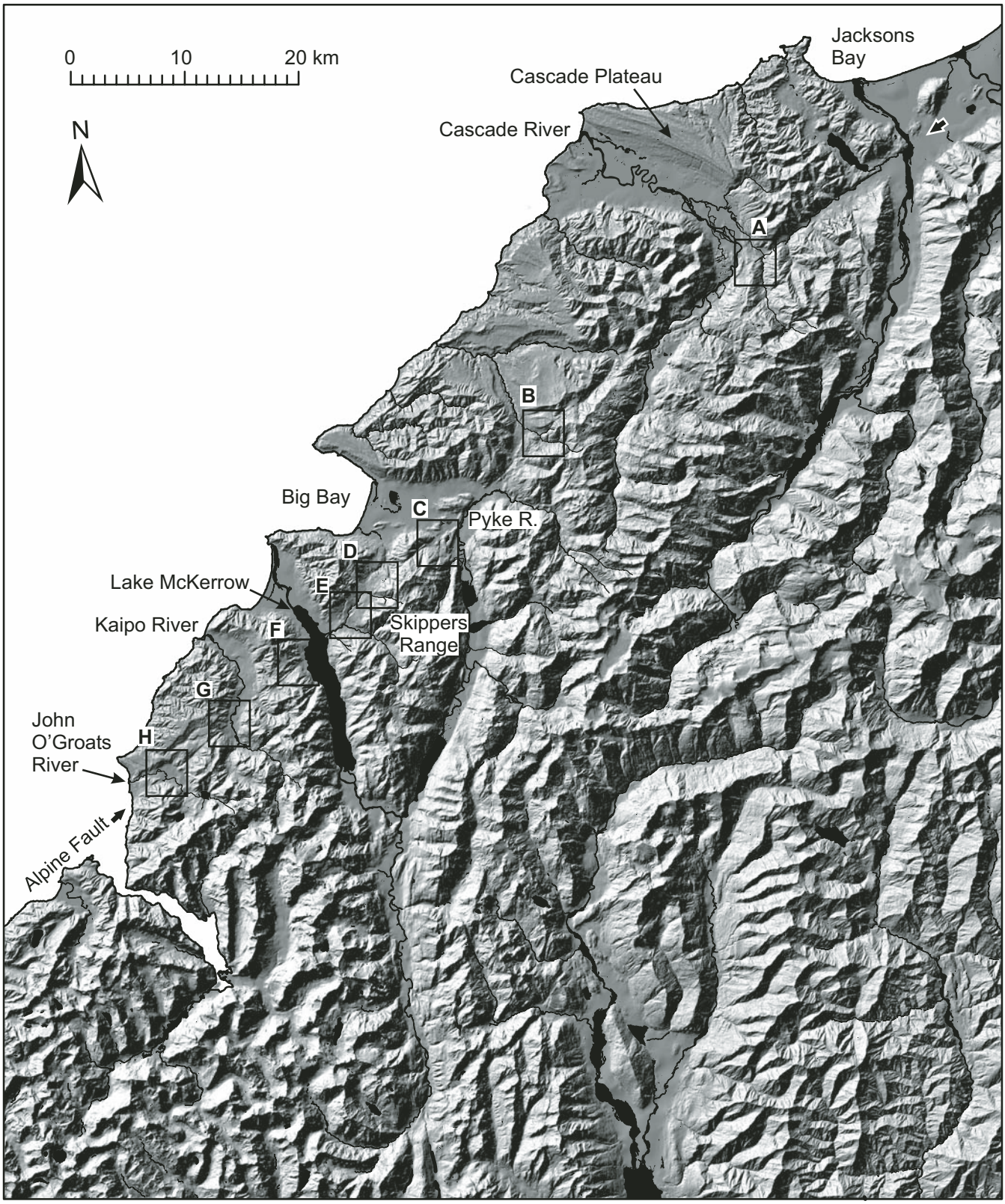

Figure 2. Topography of the study region around the southern onshore Alpine fault (derived from NZMS 260 data) illuminated from the northwest. Boxes A–H show location of offset features used in this study (Fig. 3).

TABLE 1. SYNTHESIS OF OFFSET FEATURES

Offset feature	Rank	Age (cal. ka)	C_t† (cal. ka)	Offset (m)	C_x† (m)	Rate (mm/yr)	Markers to determine offset
Martyr, SW spur	1	18	1	433	61	24.1	SW spur edge-moraine crest; NE spur edge; 140 m contour
Jerry, NE	1	18	1	475	139	26.4	440, 500, 540 m contours
Jerry, SW	1	18	1	447	104	24.8	480, 420 m contours; valley center
Hokuri north, lateral moraines	1	18	1	409	19	22.7	SW moraine crest; NE moraine crest; valley center
McKerrow, SW	1	18	1	438	73	24.3	100, 140, 180 m contours
Kaipo, SW	1	18	1	439	49	24.4	100, 140, 180 m contours
John O'Groats, NE	1	18	1	390	34	21.7	180, 240, 300 m contours
John O'Groats, SW	1	18	1	454	46	25.2	140, 180, 220 m contours
Webb Creek aggradation fan	1b	22	2	510	90	23.2	SW edge; center; NE edge
Big Bay–Pyke, SW	2	58	5	1232	48	21.2	220, 280, 340 m contours
Hokuri south, younger terminal moraine	2	58	5	1240	160	21.4	SW edge-outcrop; NE edge-outcrop; best reconstruction to valley geometry
Hokuri north, oldest moraine (D)	3	79	8	1900	100	24.1	NE moraine crest; incised creek-valley center; min. offset to NE side of valley
Hokuri south, older terminal moraine	3	79	8	1800	100	22.8	Alternate correlations: min., central, max offset.

†Confidence interval half-width (see text). C_t is age uncertainty, C_x is offset uncertainty, cal. is calendar.

from 120 m at their western limit to 340 m at the northern end of the beach (Fig. 2). The much larger Alpine fault offset here than that observed at the Martyr and Jerry Valleys (Table 1) suggests that hillslopes formed here during an earlier glacial advance. Preservation of the larger offset has been achieved by the rather complex geometry of the catchment, particularly its dual-outlet nature, which has resulted in spatially varying erosion patterns during glacial advances with different ice thicknesses. The dynamics of ancient glacier flow between the upper Pyke River and Big Bay were complicated by three factors: (1) an alternative outlet through the lower Pyke River and Lake McKerrow, (2) interactions with glaciers that filled tributary valleys (Fig. 2), and (3) several physical obstructions of height 190–407 m near the Alpine fault and immediately north of the Skippers Range (Fig. 2).

Hokuri Creek, North Branch Moraines

The north branch of Hokuri Creek lies in a short, steep, and narrow valley (500 m wide) that drains across the Alpine fault at the saddle between Big Bay and Lake McKerrow (Fig. 3D). Southeast of the Alpine fault, the northern side of the valley has a prominent lateral moraine that is offset and truncated by the fault (Sutherland and Norris, 1995; Wellman and Wilson, 1964). The southern side of the valley has a lateral moraine that is recognizable to within 100 m of the fault, where it is buried by younger alluvium. Only minor tributaries to McKenzie Creek exist to the northeast, so moraines are moderately well preserved at Alpine fault offsets of <1800 m (Sutherland and Norris, 1995).

Northwest of the Alpine fault, correlatives of both lateral moraines are recognizable in the field and on air photos with a horizontal offset of 409 ± 19 m. Vertical displacement of the northern moraine crest is irresolvable with available data and is <20 m. Lateral moraines trapped the active channel draining the small cirque at the headwaters of what is now called the north branch of Hokuri Creek. The channel between the moraines drains into McKenzie Creek; offset on the Alpine fault has resulted in the headwaters being captured by Hokuri Creek (Fig. 3D). Capture has left moraines flanking an underfit stream that is dry in its upper reaches during normal flow. Moraine geometry suggests that ice thickness was ~50 m at the Alpine fault and extended 200–400 m northwest of the Alpine fault at the time of glacial advance.

Sutherland and Norris (1995) speculated that mounds farther northeast were also offset moraines from the same catchment. In particular, mounded, bouldery topography offset 600 m from the northern edge of the valley is causing a small creek to be dextrally diverted (Fig. 3D). More speculative mounds with offsets of 1150, 1450, and 1900 m may also correlate with mounds offset from the northern edge of the valley, but moraines offset from the southern edge may also be preserved. Alternatively, some of the rather subtle mounding at 1150 and 1450 m could be related to younger landslide and fluvial deposits.

The spur at 1900 m offset, moraine D of Sutherland and Norris (1995), is larger than moraines offset by 409 ± 19 m and has been partly eroded at its northeastern edge by a tributary of McKenzie Creek. An underfit stream valley adjacent to moraine D has similar morphology to the underfit valley offset by 409 m. We used moraine D and the adjacent underfit stream to determine an offset (Fig. 3D).

We suggest that the location of a creek 1200 m northeast of the active branch of Hokuri Creek may also be controlled by moraines. We did not use the creek geometry or adjacent mounded features to compute surface displacement rate, because substantial uncertainty surrounds their geomorphic interpretation. However, the inferred offset is similar to that of glaciated hillslopes at the northern end of the Skippers Range and moraines associated with the south branch of Hokuri Creek.

Hokuri Creek, South Branch Moraines

The south branch of Hokuri Creek has one of the most spectacular exposures of the Alpine fault in South Westland (Hull and Berryman, 1986; Sutherland and Norris, 1995; Wellman and Wilson, 1964). The fault is subvertical with slickensides and corrugations that plunge 0°–5° southwest (Sutherland and Norris, 1995). Two end moraines northwest of the Alpine fault have topographic and vegetation expression; the younger glacial advance partially destroyed the older moraine (Fig. 3E). An underfit channel cutting through the younger end moraine is now abandoned, and the main channel of Hokuri Creek drains at the southern edge of the valley. Abandonment of the channel probably occurred during the last couple of slip events (Alpine fault earthquakes), and good exposures have been created as the new channel rapidly incised (Sutherland and Norris, 1995).

Southeast of the Alpine fault, a sequence of lateral moraines on the northern side of the valley has been partially eroded by fluvial processes. The inner edge of the lateral moraines is inferred to correlate with the inner edge of the end moraine and is offset 1400 m. An alternative correlation with hummocky topography inside the end moraine implies a smaller offset. On the south side of the valley, diamictite is exposed in a small tributary on the outer edge of a meander bend, where a moraine is inferred to have laterally constrained Webb Creek (Fig. 3E), and Hokuri Creek is filled with erratic boulders, suggesting a lag deposit from moraine erosion. Correlation between the eroded moraine at the Hokuri Creek meander bend and the southern Alpine fault truncation of the end moraine implies an offset of 1080 m. The best fit to observations on both sides of the valley involves an offset of 1240 m, and restoration of this offset results in the end

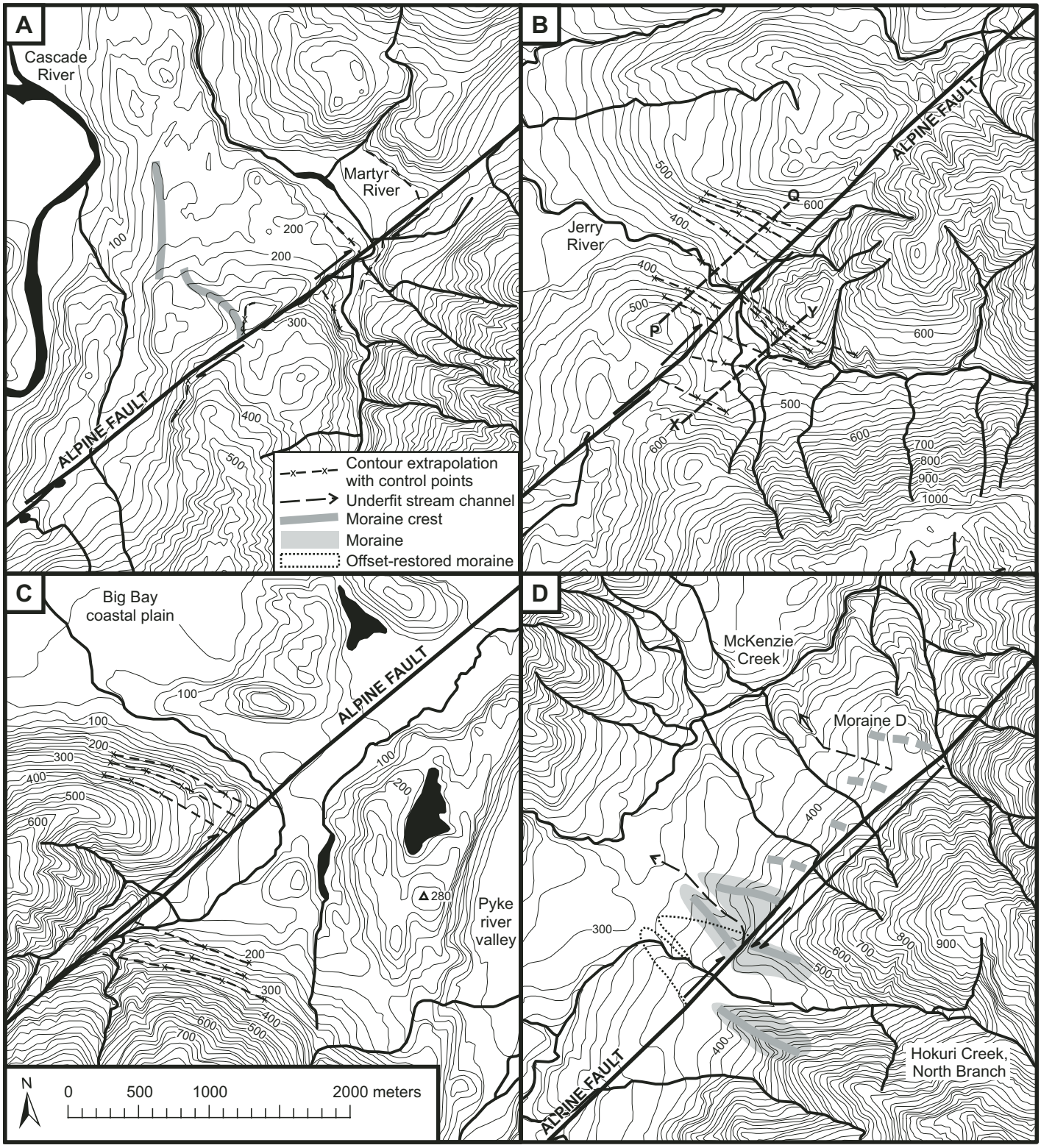

Figure 3 (*on this and following page*). Locality maps of the Alpine fault at Martyr River (A), Jerry River (B), Big Bay–Pyke River (C), north branch of Hokuri Creek (D), south branch of Hokuri Creek (E), Lake McKerrow (F), Kaipo River (G), and John O'Groats River (H). Selected moraines discussed in text are shaded.

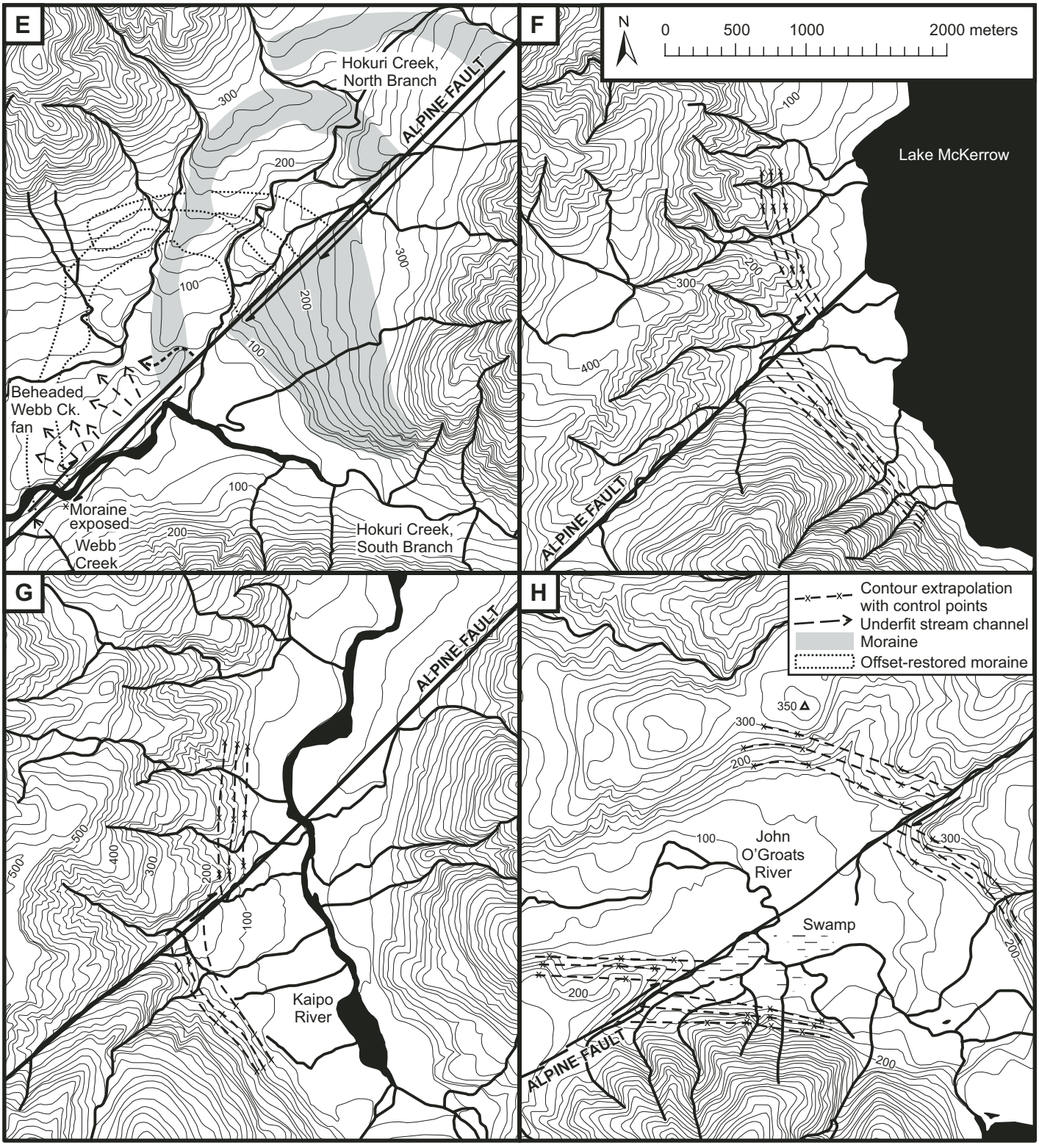

Figure 3 (*continued*). Profiles X–Y and P–Q at Jerry River (B) are shown in Figure 4. Contours are at 20 m interval and taken from NZMS 260 topographic maps (Land Information New Zealand). True north is 4° west of projected north (New Zealand Map Grid). For location see Figure 2.

moraine being relocated central to the valley headwaters (dotted in Fig. 3E). The difference in altitude between the northeastern part of the end moraine and the correlative lateral moraine is probably due to partial removal of the lateral moraine by fluvial erosion.

The outer end moraine indicates an earlier advance of similar extent to the inner moraine. It must correlate with one of the older lateral moraines on the north side of the valley, which requires an offset in the range of 1700–1900 m.

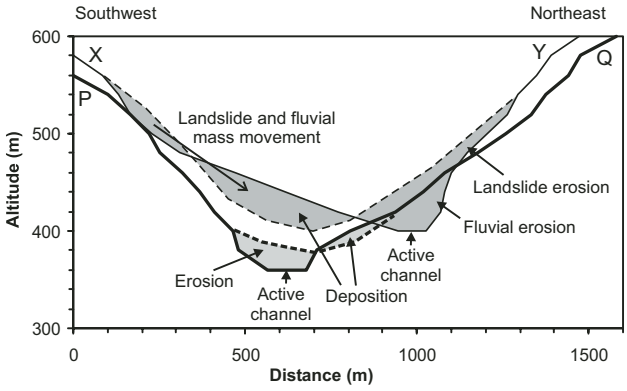

Figure 4. Profiles across Jerry River, showing the extent of hillslope modification through postglacial erosion and deposition. Dashed lines are an estimate of the original glacial hillslope. Location of profiles is given in Figure 3B, and derived offset measurements are listed in Table 1. Most uncertainty in displacement arises from the relatively large degree of surface modification southeast of the Alpine fault (profile X–Y).

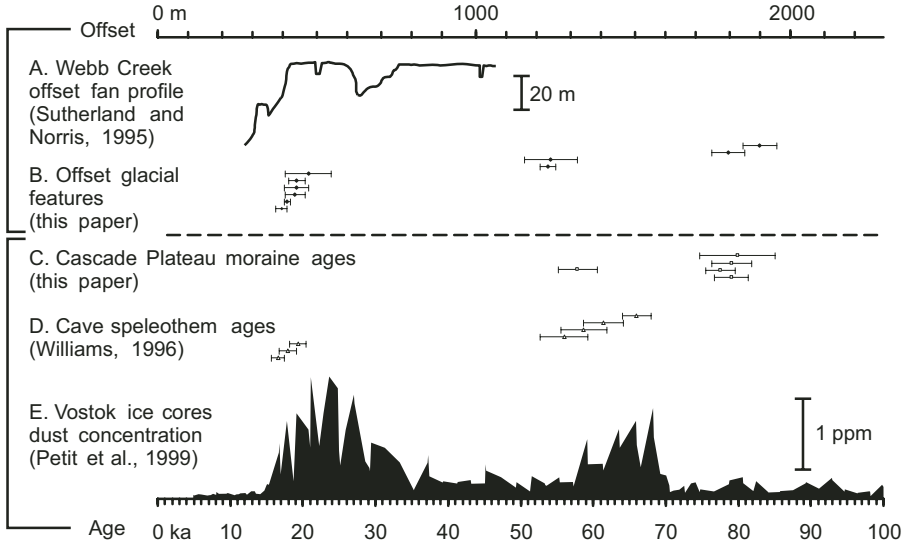

Figure 5. Offset-age correlations at a displacement rate of 23 mm/yr. (A) The offset Webb Creek fan surface height is correlated with cold climate. (B) Offset glacial landforms from different catchments record times when ice retreated across the Alpine fault (Table 1). (C) The ages of Cascade Plateau moraines provide direct evidence for glacial maxima (see GSA Data Repository material [footnote one]). (D) The age of cave speleothems from south of the study area (Williams, 1996) is inferred to place a minimum age constraint on the timing of local glacial retreats. (E) The ages of high dust concentrations in ice that accumulated at Vostok, Antarctica, are a proxy for temperate Southern Hemisphere glacial maxima, particularly within South America (Petit et al., 1999).

Webb Creek Fan Surface

Webb Creek drains a small area of gneissic and cataclastic rocks on the edge of Mount Webb (1162 m), and is depositing an alluvial fan that crosses the Alpine fault. The Webb Creek fan is being actively eroded by the south branch of Hokuri Creek, but radiocarbon dates show that the main channel of Hokuri Creek was confined to a narrow gorge at the southern edge of the inner end moraine before 370 ± 150 cal. yr B.P. (Sutherland and Norris, 1995). The channel of Webb Creek southeast of the Alpine fault is constrained in a narrow erosional channel (Fig. 3E).

The fault scarp between Hokuri Creek and the truncated southern end moraine is made up of offset alluvial fan and channel deposits from Webb Creek (Fig. 3E). Fluvial morphology is clearly apparent, and several beheaded channels end at the steep fault scarp (Sutherland and Norris, 1995). Webb Creek had sufficient sediment supply before Holocene time to maintain its continuously offset fan surface at a height that was greater than the base of the gorge through the inner end moraine. Hence, the offset Webb Creek fan surface was higher than the Hokuri Creek floodplain: the fault scarp dammed the valley and constrained Hokuri Creek to pass through the gorge in end moraine. Aggradation rates dropped substantially during Holocene time, resulting in a fan surface that was lower than the Hokuri Creek floodplain, and eventual capture of Hokuri Creek occurred when this lower surface was offset adjacent to the Hokuri Creek floodplain.

The height of the offset alluvial fan can be related to changing conditions of sediment supply, which are correlated with known changes in regional climate. Offset measurements can be made with relative precision, because Webb Creek southeast of the Alpine fault was and is incised in a narrow valley. High aggradation rates are correlated with times of cold climate, when vegetation cover was less and mechanical weathering and erosion processes were more effective. Following deposition of the end moraine, high aggradation rates are apparent at offsets of 1200–900 m. At offsets of 900–650 m, aggradation rates were progressively lower, and then were high again at offsets of 600–420 m. The general reduction in fan height at offsets less than 420 m was punctuated by a narrow area of increased fan height at an offset of ~400 m, but the exact offset is difficult to determine because of Holocene erosion by Hokuri Creek. We correlate the region of high aggradation rates at offsets 600–420 m with the Last Glacial Maximum (Fig. 5).

Lake McKerrow Hillslope

The glaciated walls of the southern edge of Lake McKerrow are offset by the Alpine fault (Hull and Berryman, 1986). A plateau area at an altitude of 380–400 m probably represents a composite moraine and aggradation surface associated with a former ice level. Fluvial erosion has modified the region northwest of the Alpine fault, but sufficient morphology is preserved to determine an offset of 438 ± 73 m (Fig. 3F).

Formation of glacial wall morphology is constrained to before deposition of lake sediments that are preserved on the opposite side of the lake, at the mouth of Hokuri Creek. The lake sediments contain glacial dropstones and wood fragments dated at 13,120 ± 110 ^{14}C yr B.P. (Sutherland and Norris, 1995), equivalent to a calendar age (95% confidence interval) of 14.8–16.3 cal. ka (Stuiver et al., 1998).

Kaipo River Hillslope

The morphology of the southwest side of the Kaipo River valley is similar to that found adjacent to Lake McKerrow. The glaciated valley wall has a similar offset, but shattered rocks northwest of the fault trace have been affected by fluvial erosion (Fig. 3G).

John O'Groats Hillslopes and Moraines

Both sides of the John O'Groats Valley are offset by the Alpine fault (Fig. 3H). On the southwest side of the valley, a moraine spur that separates the valley from the mouth of Milford Sound is conspicuously offset (Cooper and Norris, 1990; Wellman, 1984). Fluvial incision of the valley wall northwest of the fault trace, and incision along the fault trace, combined with a moderately acute angle between the fault and valley wall introduce some uncertainty into the offset determination. The northeast side of the valley has a hummocky moraine plateau surface at 300–350 m altitude and an offset valley wall. Again, fluvial incision must be accounted for, and regions that have been significantly modified were excluded from the analysis (Fig. 3H).

Vertical slip on the Alpine fault will oppositely bias offset determinations on either side of the valley, because contours are used to determine horizontal offset. The swamp that lies upstream from the fault trace has been previously interpreted as resulting from horizontal offset of topography (Clark and Wellman, 1959; Wellman, 1984), but a slight upthrow on the northwest side of the fault trace may also contribute to the poor drainage in a similar fashion to that observed at Hokuri Creek and Cascade River (Berryman et al., 1992; Sutherland and Norris, 1995). Use of data from both sides of the valley ensures no net bias is introduced into any derivative slip-rate calculation.

AGE-OFFSET RELATIONSHIPS AND RANK CORRELATION

We adopt a rank correlation approach to assign ages to offset features in this paper, and hence to determine Alpine fault surface displacement rate. This approach was necessary because no features in the study region have both a clear Alpine fault offset and an objectively determined and unequivocal age. Offset glacial features fall into three groups with offsets of ~430, 1240, and 1850 m (Fig. 5). We assign offset features within each group to the same rank and assign their age by regional correlation. Valley morphology is primarily glacial in origin, and many river valleys in the western South Island have similar glacial histories (Almond et al., 2001; Suggate, 1990; Suggate and Waight, 1999; Williams, 1996).

The first offset group (430 m offset; rank 1) was formed toward the end of the Last Glacial Maximum, when ice retreated across the Alpine fault. The end of the Last Glacial Maximum in northwestern South Island occurred at 17–19 cal. ka (Suggate, 1990). This is confirmed by radiocarbon dating and high-resolution pollen stratigraphy adjacent to Mount Cook, where rapid glacial retreat commenced at ca. 18.3 cal. ka (Almond et al., 2001; Vandergoes and Fitzsimons, 2003). South of the study area, uranium series dates on cave speleothems record the onset of deglaciation after 19.1 cal. ka and before 16.6 cal. ka (Williams, 1996). Stratigraphy at the edge of Lake McKerrow, which is adjacent to the highest mountains in the region, confirms that substantial glaciers have not crossed the Alpine fault since 14.8–16.3 cal. ka (Sutherland and Norris, 1995). Additional regional correlations indicate significant climate warming at 18 ± 1 cal. ka, and this is adopted as a best estimate for the age of rank 1 offset features.

We treat the Webb Creek offset fan differently from other rank 1 offsets, because it records the entire Last Glacial Maximum period, rather than just the end of the Last Glacial Maximum. We assign an age of 22 ± 2 cal. ka to the peak of the Last Glacial Maximum (rank 1b) based upon radiocarbon and stratigraphic evidence from New Zealand (Almond et al., 2001; Suggate, 1990; Suggate and Waight, 1999) and global correlations (Petit et al., 1999; Shackleton, 2000).

The second offset group (1240 m offset; rank 2) was formed at a time when glacier ice was more extensive than during formation of the first group, but has limited extent because of widespread modification during the Last Glacial Maximum. The inner end moraine at Hokuri Creek and the glacially scoured northern edge of the Skippers Range (Pyke–Big Bay) are the only unequivocal features assigned to rank 2. Possible moraines and an underfit stream offset from the north branch of Hokuri Creek are also correlated with rank 2, but were not used to calculate surface displacement rate. Stratigraphic relationships show that maximum ice extent during the last glaciation in northwestern South Island occurred before 50 cal. ka (Suggate, 1990). Uranium series data on speleothems south of the study area indicate deglaciation was under way by 58 cal. ka, and there were possibly deglaciation events as early as 66 cal. ka (Williams, 1996). Cosmogenic data from the Cascade Plateau indicate a moraine deposition event at, or just before 58 cal. ka. This correlates with the end of a major Southern Hemisphere glacial event recorded as a time of increased dust concentration from 69 to 58 cal. ka in the Vostok ice core (Petit et al., 1999). An age of 58 ± 5 cal. ka is adopted here for rank 2 offset landforms.

The third offset group (1850 m offset; rank 3) is found at the north and south branches of Hokuri Creek, where evidence is preserved for an earlier glacial advance of similar extent to that which formed rank 2 landforms. The age of this glacial event is constrained by cosmogenic surface exposure ages from the Cascade Plateau, which indicate several moraines were deposited at ca. 79 cal. ka (Fig. 5; GSA data repository material [see footnote 1]). We assign a conservative age uncertainty of 10% (±8 k.y.) to include uncertainties in measurement and assumptions involved in the age calculation. Rank 3 landforms have restricted extent because of modification by later glacial periods and because the larger offsets have resulted in modification by adjacent catchments.

ALPINE FAULT SURFACE DISPLACEMENT RATE

Previous estimates of the Quaternary surface displacement rate along this 80 km section of the Alpine fault were based upon offset features with ~430 m offset at: Martyr River (Clark and Wellman, 1959; Wellman, 1953); Lake McKerrow and Hokuri Creek (Hull and Berryman, 1986; Sutherland and Norris, 1995); and John O'Groats River (Wellman, 1984). We have estimated bounding values of age and offset at all catchments in the study area, but we do not have a consistent basis for inferring the shape of the offset or age probability density functions. We assume the simplest model: any value

TABLE 2. DISPLACEMENT RATE SUMMARY STATISTICS

Distribution	Mean	Standard deviation	Min* (95%)	Max* (95%)
Rank 1	24.2	1.2	22.1	26.5
Rank 1b	23.2	2.7	18.6	28.4
Rank 2	21.4	1.4	18.9	24.0
Rank 3	23.5	1.5	21.0	26.3
Joint probability	23.1	0.7	21.6	24.5
Weighted mean	23.2	0.7	21.8	24.6
Arithmetic mean	23.1	0.9	21.4	24.8

*Bracketing values for 95% confidence interval.

within the confidence interval of an observation (defined by the bounding values; Table 1) is equally likely, and the probability is zero outside the confidence interval. Values close to the mean generally have higher probability, and hence the assumption of equal probability is conservative, because it leads to overestimation of the variance of the offset or age probability distribution.

The uncertainties in age for features of similar offset are assumed to be perfectly correlated between different localities (features of the same rank are assumed to be the same age), and offset determinations for features of the same age are assumed to be independent. We combine offset data by rank and compute the resulting probability density function for surface displacement rate by dividing by the age (see GSA Data Repository material [see footnote 1]). The assumption of independent offset measurements is reasonable, because offset data are from different catchments. The assumption that features of the same offset rank are the same age can only lead to an overestimation of the variance in rate, because any Alpine fault surface displacement (earthquakes) during deglaciation would lead to positive age offset correlation within the rank, similar to the longer-term trend that is demonstrated by data from different ranks.

On the basis of our observations, offset measurement imprecision is much larger than real differences in offset between catchments, i.e., the assumption of negligible age offset correlation within rank 1 offset data is justified. The timing of glacial retreat in one valley is the same on either side, so the true offset should be the same, but differences in measured offset within the John O'Groats River valley are 64 m. The timing of glaciation in catchments with similar hypsometry is expected to be similar, but the measured difference between sites at Jerry River and the north branch of Hokuri Creek, which are similar (GSA Data Repository material [see footnote 1]), is 69 m.

We computed a slip-rate probability density function from data of each rank, and we then combined these independent estimates to determine a single slip-rate probability density function. Full details are given in the GSA data repository (see footnote 1). The method used to combine displacement rate probability distributions for different ranks has little effect on the conclusion (Table 2; GSA Data Repository [see footnote 1]). This is intuitively expected, because it is likely that the true surface displacement rate has changed little, when averaged over 80 k.y., and 17 probability distributions have been combined to arrive at the result.

From the individual and combined results, we test the hypothesis: are surface displacement rates computed from each rank significantly different from the mean surface displacement rate? The joint frequency of the weighted mean surface displacement rate and that derived from ranks 1, 1b, 2, and 3 are, respectively, 22.0%, 12.2%, 13.4%, and 21.3%, which is a measure of how much the pair of probability density functions overlaps. If the weighted mean is taken as the null hypothesis, what percentage of randomly drawn data sets would fit the observations? The results above indicate that there is no significant variation in surface displacement rate (at 1%, 5%, or 10% level) when it is computed over different time intervals (Fig. 6).

We conclude that the mean surface displacement rate of 23.1–23.2 mm/yr, as computed from displacements that accumulated over the time interval 79–18 ka, is insensitive to the method used to combine data, and that the surface displacement rate is constrained (at 95% confidence level) not to have varied, or be in error, by more than 1.7 mm/yr for this section of the Alpine fault when averaged over time intervals >18 k.y. Assumptions of rectangular probability density functions at each site and no age offset correlation within rank are conservative in that they overestimate uncertainty, and the true confidence level is >95%. This is supported by an analysis of variance of rank 1 offsets (GSA Data Repository [see footnote 1]).

A constant mean surface displacement rate, when it is computed over time intervals of at least several thousand years, is supported by observations of offset Holocene river terraces (Norris and Cooper, 2001) and offset Pliocene conglomerates (Sutherland et al., 1995). A constant mean surface displacement rate is expected, when it is computed over time intervals of at least several thousand years, because all the displacement rate determinations are based on offsets that are much larger than the 8–9 m coseismic displacements, and the measured offsets accumulated over time intervals much greater than the Alpine fault's typical earthquake recurrence interval of 300–400 yr (Berryman et al., 1992; Hull and Berryman, 1986; Sutherland and Norris, 1995).

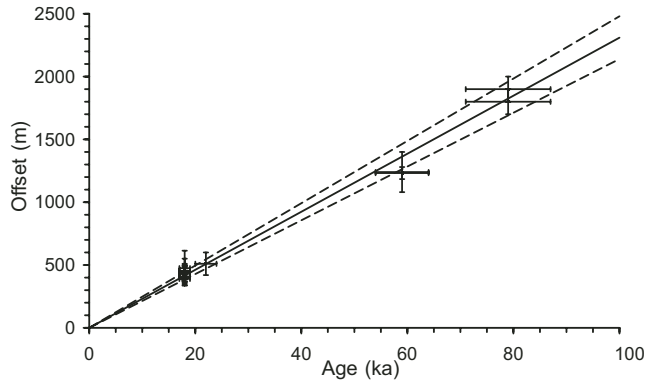

Figure 6. Graph showing age and offset for individual sites (Table 1). Error bars are the respective C_x and C_t values. The constant displacement rate line and 95% confidence interval is 23.1 ± 1.7 mm/yr, derived from the arithmetic mean of displacement rates computed for each rank (Table 2).

SEISMIC HAZARD

Our Alpine fault surface displacement rate determination is ~3 mm/yr lower than previous estimates, but falls within the confidence intervals of earlier estimates (Berryman et al., 1992; Clark and Wellman, 1959; Norris and Cooper, 2001; Sutherland and Norris, 1995; Wellman, 1984). The lower Alpine fault slip rate estimate and reduction in slip rate uncertainty results in only a slight reduction in predicted seismic hazard for the Alpine fault (details in GSA Data Repository material [see footnote 1]). The hazard remains high, with a 14%–29% model-dependent chance of rupture in the next 50 yr, reduced from earlier estimates of 15%–35% (Rhoades and Van Dissen, 2003). A more significant implication of the reduction in Alpine fault surface displacement

rate is that the residual plate motion is greater than previously thought, and hence seismic hazard may be higher than previously thought elsewhere within the plate boundary zone.

PARTITIONING OF PLATE BOUNDARY MOTION

The southern onshore Alpine fault is pure strike slip in character, but plate boundary motion is obliquely convergent; NUVEL-1A Australia-Pacific relative plate motion computed for a location at Lake McKerrow is 36.2 ± 3 mm/yr along azimuth 067.5 ± 2° (DeMets et al., 1994). Motion of 23.1 ± 1.7 mm/yr in the direction 052° is accommodated by slip on the Alpine fault, and residual plate motion of 15 ± 4 mm/yr in direction 091 ± 2° must be accommodated elsewhere (Fig. 1). All uncertainties are calculated at a 95% confidence level.

At the eastern and western limits of deformation in the southern South Island, reverse faults strike approximately parallel to the Alpine fault (Fig. 1), but are inferred to have relatively low rates and only a minor strike-slip component (Barnes et al., 2002; Beanland and Berryman, 1989; Jackson et al., 1996; Nathan et al., 1986). The combined rate of Quaternary deformation on faults at the eastern and western peripheries of the plate boundary is inferred to be 3–8 mm/yr: that is 20%–50% of the plate motion that is unaccounted for after Alpine fault plate motion is subtracted from the NUVEL-1A rate. The remaining plate motion is accommodated within a region 80 km southeast of the Alpine fault and must range between 13 mm/yr in direction 080° and 11 mm/yr in direction 061° (Fig. 1).

The region southeast of the Alpine fault has elevated topography, high geodetic strain, high levels of shallow seismicity, and faults and folds have been rotated to a dominant strike of ~020° by accumulated finite strain (Anderson and Webb, 1994; Beavan and Haines, 2001; Norris, 1979; Sutherland, 1999). For realistic minimum and maximum figures of 3 mm/yr and 8 mm/yr of shortening at the periphery of the plate boundary, the residual plate motion calculation predicts obliquities of slip on faults <80 km southeast of the Alpine fault to be 30° (11 mm/yr shortening, 7 mm/yr dextral) and 49° (7 mm/yr shortening, 8 mm/yr dextral), respectively. The predicted obliquity and rate of fault slip is reduced if clockwise vertical-axis block rotation is also taking place.

An observed transition in Quaternary structural style in the transitional region 80 km southeast of the Alpine fault (Beanland and Barrow-Hurlbert, 1988; Beanland and Berryman, 1989) supports the inference that dextral-reverse slip becomes significant near to the Alpine fault. We conclude that the 80-km-wide zone southeast of the Alpine fault has cumulative strike-slip rates in the range of 7–8 mm/yr, shortening rates in the range of 11–7 mm/yr, and that clockwise fault block rotation may play a significant role in accommodating plate boundary strain.

CONCLUSIONS

Based on analysis of offset Quaternary landforms along an 80 km fault section, the Alpine fault surface displacement rate is 23.1 mm/yr, with standard error 0.8 mm/yr, and 95% confidence interval half-width 1.7 mm/yr. Our surface displacement rate estimate is 3 mm/yr lower and has a confidence interval one-third the size of earlier analyses (Berryman et al., 1992; Clark and Wellman, 1959; Norris and Cooper, 2001; Sutherland and Norris, 1995; Wellman, 1984). The lower displacement rate estimate only slightly reduces Alpine fault seismic hazard, which remains high: there is a 14%–29% model-dependent chance of rupture in the next 50 yr.

The precise definition of Alpine fault slip rate allows us to infer how residual plate boundary motion is accommodated across the 300 km width of southern South Island, and we can relate that to the regional tectonic setting (Fig. 7). The location and trend of the Alpine fault are inherited from an Eocene passive margin that was displaced into the South Island continent during late Cenozoic time (Sutherland et al., 2000). Ocean crust adjacent to this passive margin has been subducted and has localized strain at depth:

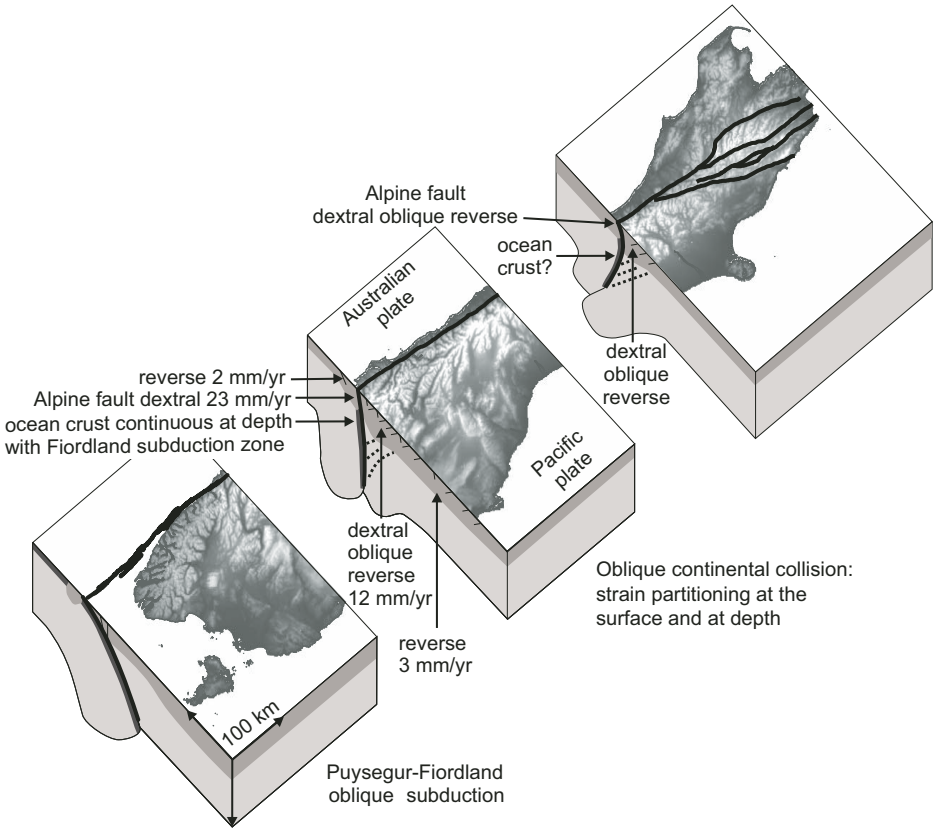

Figure 7. Kinematic model for southern New Zealand. Australian plate oceanic crust is obliquely subducted at the Puysegur-Fiordland subduction zone, and crustal deformation is restricted to a zone <80 km southeast of the subduction thrust. Oblique continental collision occurs in southern South Island, but a steeply dipping Wadati-Benioff zone at depth attests to deep-seated strain partitioning. The steeply dipping plate boundary at depth is inferred to be continuous with 23 mm/yr of strike-slip motion on the Alpine fault. A zone of dextral-oblique reverse faulting and block rotation <80 km southeast of the Alpine fault accommodates 12 mm/yr of plate motion and overlies a zone of incipient subduction of Pacific mantle. Shortening of 5 mm/yr at the peripheries of the plate boundary may be related to distributed lithospheric shortening or crustal detachment. In central South Island, crustal plate motion occurs by oblique reverse movement on the Alpine fault and block rotations and oblique reverse faulting in a zone 80 km southeast of the Alpine fault.

a steeply dipping Wadati-Benioff zone exists in the southern part of the study area and farther to the south at the Puysegur-Fiordland subduction zone (Eberhart-Phillips and Reyners, 2001; Reyners et al., 2002). A Wadati-Benioff zone is not present in the northern part of the study area or in central South Island (Eberhart-Phillips, 1995), though plate reconstructions indicate that ocean crust was previously attached at least as far north as Mount Cook (Sutherland et al., 2000). The three-dimensional nature of the South Island plate boundary requires a transition from Australian plate subduction in the south to Pacific plate subduction in the north.

The steeply dipping plate interface inferred from seismicity at depth is poorly oriented to accommodate convergent motion, but well oriented to accommodate the much larger strike-slip component of plate boundary motion. We suggest that the interface at depth is continuous with 23 mm/yr of surface strike-slip motion on the Alpine fault (Fig. 7). Oblique reverse faults and block rotations within an 80-km-wide zone southeast of the Alpine fault accommodate 11–13 mm/yr (±4 mm/yr) of plate motion that may be related to incipient subduction of Pacific plate mantle and distributed mantle shear close to the plate interface (Fig. 7). A rate of 3–8 mm/yr of shortening on reverse faults at the eastern and western peripheries of the plate boundary zone is associated with crustal detachment or distributed shortening of the entire lithosphere.

ACKNOWLEDGMENTS

We thank Kyeong Kim, Albert Zondervan, and Mauri McSaveney for agreeing to let us include Cascade Plateau cosmogenic isotope results in the GSA Data Repository material; David Rhoades for computing probabilities of Alpine fault rupture; Biljana Lukovic for geographic information system (GIS) assistance; David Rhoades, Russ Van Dissen, K. Sieh, and J.-P. Avouac for helpful comments on an earlier version of the manuscript; and Harvey Kelsey, Don Easterbrook, and Bill Bull for their constructive reviews. This work was funded by the New Zealand Foundation for Research Science and Technology and assisted by a Visiting Associate award from the California Institute of Technology.

REFERENCES CITED

Almond, P.C., Moar, N.T., and Lian, O.B., 2001, Reinterpretation of the glacial chronology of South Westland, New Zealand: New Zealand Journal of Geology and Geophysics, v. 44, no. 1, p. 1–15.

Anderson, H., and Webb, T., 1994, New Zealand seismicity: Patterns revealed by the upgraded National Seismograph Network: New Zealand Journal of Geology and Geophysics, v. 37, p. 477–493.

Barnes, P.M., Sutherland, R., Davy, B., and Delteil, J., 2001, Rapid creation and destruction of sedimentary basins on mature strike-slip faults: An example from the offshore Alpine fault, New Zealand: Journal of Structural Geology, v. 23, p. 1727–1739, doi: 10.1016/S0191-8141(01)00044-X.

Barnes, P.M., Davy, B., Sutherland, R., and Delteil, J., 2002, Frontal accretion and thrust wedge evolution under very oblique plate convergence: Fiordland Basin, New Zealand: Basin Research, v. 14, p. 439–466, doi: 10.1046/j.1365-2117.2002.00178.x.

Beanland, S., and Barrow-Hurlbert, S.A., 1988, The Nevis-Cardrona fault system, central Otago, New Zealand; late Quaternary tectonics and structural development: New Zealand Journal of Geology and Geophysics, v. 31, no. 3, p. 337–352.

Beanland, S., and Berryman, K.R., 1989, Style and episodicity of late Quaternary activity on the Pisa-Grandview fault zone, central Otago, New Zealand: New Zealand Journal of Geology and Geophysics, v. 32, no. 4, p. 451–461.

Beavan, J., and Haines, J., 2001, Contemporary horizontal velocity and strain rate fields of the Pacific-Australian plate boundary zone through New Zealand: Journal of Geophysical Research, v. 106, no. 1, p. 741–770, doi: 10.1029/2000JB900302.

Beavan, J., Moore, M., Pearson, C., Henderson, M., Parsons, B., Bourne, S., England, P., Walcott, R.I., Blick, G., Darby, D., and Hodgkinson, K., 1999, Crustal deformation during 1994–98 due to oblique continental collision in the central Southern Alps, New Zealand, and implications for seismic potential of the Alpine fault: Journal of Geophysical Research, v. 104, no. B11, p. 25,233–25,255, doi: 10.1029/1999JB900198.

Berryman, K.R., Beanland, S., Cooper, A.F., Cutten, H.N., Norris, R.J., and Wood, P.R., 1992, The Alpine fault, New Zealand: Variation in Quaternary structural style and geomorphic expression: Annales Tectonicae, v. 6, p. 126–163.

Clark, R.H., and Wellman, H.W., 1959, The Alpine fault from Lake McKerrow to Milford Sound: New Zealand Journal of Geology and Geophysics, v. 2, p. 590–601.

Cooper, A.F., and Norris, R.J., 1990, Estimates for the timing of the last coseismic displacement on the Alpine fault, northern Fiordland, New Zealand: New Zealand Journal of Geology and Geophysics, v. 33, no. 2, p. 303–307.

Delteil, J., Collot, J.-Y., Wood, R., Herzer, R., Calmant, S., Christoffel, D., Coffin, M., Ferriere, J., Lamarche, G., Lebrun, J.-F., Mauffret, A., Pontoise, B., Popoff, M., Ruellan, E., Sosson, M., and Sutherland, R., 1996, From strike-slip faulting to oblique subduction: A survey of the Alpine fault–Puysegur Trench transition, New Zealand; results of cruise Geodynz-sud leg 2: Marine Geophysical Researches, v. 18, p. 383–399, doi: 10.1007/BF00286086.

DeMets, C., Gordon, R.G., Argus, D.F., and Stein, S., 1994, Effect of recent revisions to the geomagnetic time scale on estimates of current plate motions: Geophysical Research Letters, v. 21, p. 2191–2194, doi: 10.1029/94GL02118.

Eberhart-Phillips, D., 1995, Examination of seismicity in the central Alpine fault region, South Island, New Zealand: New Zealand Journal of Geology and Geophysics, v. 38, p. 571–578.

Eberhart-Phillips, D., and Reyners, M., 2001, A complex, young subduction zone imaged by three-dimensional seismic velocity, Fiordland, New Zealand: Geophysical Journal International, v. 146, p. 731–746, doi: 10.1046/j.0956-540x.2001.01485.x.

Hull, A.G., and Berryman, K., 1986, Holocene tectonism in the region of the Alpine fault at Lake McKerrow, Fiordland, New Zealand: Royal Society of New Zealand Bulletin, v. 24, p. 317–331.

Jackson, J., Norris, R., and Youngson, J., 1996, The structural evolution of fault and fold systems in central Otago, New Zealand: Evidence revealed by drainage patterns: Journal of Structural Geology, v. 18, p. 217–234, doi: 10.1016/S0191-8141(96)80046-0.

Nathan, S., Anderson, H.J., Cook, R.A., Herzer, R.H., Hoskins, R.H., Raine, J.I., and Smale, D., 1986, Cretaceous and Cenozoic sedimentary basins of the West Coast Region, South Island: Wellington, New Zealand Geological Survey Basin Studies, Department of Scientific and Industrial Research, 90 p.

Norris, R.J., 1979, A geometrical study of finite strain and bending in the South Island: Royal Society of New Zealand Bulletin, v. 18, p. 21–28.

Norris, R.J., and Cooper, A.F., 2001, Late Quaternary slip rates and slip partitioning on the Alpine fault, New Zealand: Journal of Structural Geology, v. 23, no. 2–3, p. 507–520, doi: 10.1016/S0191-8141(00)00122-X.

Norris, R.J., Koons, P.O., and Cooper, A.F., 1990, The obliquely-convergent plate boundary in the South Island of New Zealand; implications for ancient collision zones: Journal of Structural Geology, v. 12, no. 5–6, p. 715–725, doi: 10.1016/0191-8141(90)90084-C.

Petit, J.R., Jouzel, J., Raynaud, D., Barkov, N.I., Barnola, J.M., Basile, I., Bender, M., Chappellaz, J., Davis, M., Delaygue, G., Delmotte, M., Kotlyakov, V.M., Legrand, M., Lipenkov, V.Y., Lorius, C., Pepin, L., Ritz, C., Saltzmann, E., and Stievenard, M., 1999, Climate and atmospheric history of the past 420,000 years from the Vostok ice core, Antarctica: Nature, v. 399, no. 6735, p. 429–436, doi: 10.1038/20859.

Reyners, M., Robinson, R., Pancha, A., and McGinty, P., 2002, Stresses and strains in a twisted subduction zone—Fiordland, New Zealand: Geophysical Journal International, v. 148, p. 637–648, doi: 10.1046/j.1365-246X.2002.01611.x.

Rhoades, D.A., and Van Dissen, R.J., 2003, Estimates of time-varying hazard of rupture of the Alpine fault, New Zealand, allowing for uncertainties: New Zealand Journal of Geology and Geophysics, v. 46, p. 479–488.

Shackleton, N.J., 2000, The 100,000-year ice-age cycle identified and found to lag temperature, carbon dioxide, and orbital eccentricity: Science, v. 289, no. 5486, p. 1897–1902, doi: 10.1126/science.289.5486.1897.

Stuiver, M., Reimer, P.J., Bard, E., Beck, J.W., Burr, G.S., Hughen, K.A., Kromer, B., McCormac, G., van der Plicht, J., and Spurk, M., 1998, INTCAL98 radiocarbon age calibration, 24,000–0 cal B.P.: Radiocarbon, v. 40, no. 3, p. 1041–1083.

Suggate, R.P., 1990, Late Pliocene and Quaternary glaciations of New Zealand: Quaternary Science Reviews, v. 9, no. 2–3, p. 175–197, doi: 10.1016/0277-3791(90)90017-5.

Suggate, R.P., and Waight, T.E., 1999, Geology of the Kumara-Moana area, Institute of Geological and Nuclear Sciences Geological Map 24: Lower Hutt, New Zealand, Institute of Geological and Nuclear Sciences, scale 1:50,000.

Sutherland, R., 1994, Displacement since the Pliocene along the southern section of the Alpine fault, New Zealand: Geology, v. 22, no. 4, p. 327–330, doi: 10.1130/0091-7613(1994)022<0327:DSTPAT>2.3.CO;2.

Sutherland, R., 1999, Cenozoic bending of New Zealand basement terranes and Alpine fault displacement: A brief review: New Zealand Journal of Geology and Geophysics, v. 42, p. 295–301.

Sutherland, R., and Norris, R.J., 1995, Late Quaternary displacement rate, paleoseismicity and geomorphic evolution of the Alpine fault: Evidence from near Hokuri Creek, South Westland, New Zealand: New Zealand Journal of Geology and Geophysics, v. 38, p. 419–430.

Sutherland, R., Nathan, S., Turnbull, I.M., and Beu, A.G., 1995, Pliocene-Quaternary sedimentation and Alpine fault–related tectonics in the lower Cascade Valley, South Westland, New Zealand: New Zealand Journal of Geology and Geophysics, v. 38, no. 4, p. 431–450.

Sutherland, R., Davey, F., and Beavan, J., 2000, Kinematics of plate boundary deformation in South Island, New Zealand, is related to inherited lithospheric structure: Earth and Planetary Science Letters, v. 177, p. 141–151, doi: 10.1016/S0012-821X(00)00043-1.

Vandergoes, M.J., and Fitzsimons, S.J., 2003, The last glacial–interglacial transition (LGIT) in South Westland, New Zealand: Paleoecological insight into mid-latitude Southern Hemisphere climate change: Quaternary Science Reviews, v. 22, p. 1461–1476, doi: 10.1016/S0277-3791(03)00074-X.

Wellman, H.W., 1953, Data for the study of Recent and late Pleistocene faulting in the South Island of New Zealand: New Zealand Journal of Science and Technology, no. B34, p. 270–288.

Wellman, H.W., 1984, The Alpine fault, New Zealand, near Milford Sound and to the southwest: Geological Magazine, v. 121, p. 437–441.

Wellman, H.W., and Wilson, A.T., 1964, Notes on the geology and archaeology of the Martins Bay district: New Zealand Journal of Geology and Geophysics, v. 7, p. 702–721.

Williams, P.W., 1996, A 230 ka record of glacial and interglacial events from Aurora Cave, Fiordland, New Zealand: New Zealand Journal of Geology and Geophysics, v. 39, no. 2, p. 225–241.

Manuscript Received by the Society 22 April 2004
Revised Manuscript Received 9 August 2005
Manuscript Accepted 25 August 2005

Printed in the USA

Geological Society of America Bulletin

Quaternary slip rate and geomorphology of the Alpine fault: Implications for kinematics and seismic hazard in southwest New Zealand

Rupert Sutherland, Kelvin Berryman and Richard Norris

Geological Society of America Bulletin 2006;118, no. 3-4;464-474
doi: 10.1130/B25627.1